communications earth & environment

Article

https://doi.org/10.1038/s43247-024-01803-y

Greening urban areas in line with population density and ecological zone can reduce premature mortality

Michael D. Garber[1,2] ✉, Tarik Benmarhnia[1,3], Weiqi Zhou[4,5,6], Pierpaolo Mudu[7,8] & David Rojas-Rueda[2,9]

Urban green space and urban compactness are each important principles for designing healthy, climate-resilient cities. The principles can co-exist, but greening may come at density's expense if not considered deliberately. Existing studies estimating health impacts of greening scenarios have not considered what level of greenness is attainable for different population densities. Here, using the square kilometer as the unit of analysis, we estimate non-accidental mortality that could be prevented among adults older than 30 by greening that small area to a level of greenness assumed to be attainable based on its broader urban area (N = 15,917 globally), population density, and ecological zone. Results suggest a large potential for urban greening even in the most population-dense parts of cities such that on average 54 deaths per 100,000 could be prevented per year in those areas. That estimate may be about 25% higher or lower due to uncertainty in the underlying model.

As the world's population becomes more urban[1], urban design plays an ever-more important role in human health[2]. Among the several urban-planning-related actions that can support population health[3–5], two include the provision of accessible urban green space and compactness, that is, designing cities in a dense manner[3]. As reviews on this topic describe[6–9], exposure to urban green space can mitigate exposure to urban heat, improve air quality[10], sequester carbon[11], encourage physical activity and socialization, and improve mental health[12]. Through these and other mechanisms, exposure to urban green space may prevent premature mortality[13]. City compactness, often measured by population density, can also lead to myriad health benefits for residents[3,14,15]. For one, compact cities, exemplified by the European 15-minute-city model[16,17], encourage active transportation (e.g., walking, bicycling, and rolling)[4,18], which has individual- and community-level benefits, including increased physical activity and reduced greenhouse gas emissions[19]. Combined with other policy measures like zoning reform, compactness can also ease constraints on housing supply, thereby improving housing affordability, assuming housing is market-priced[20,21]. Finally, denser cities may use less energy from the transportation[22] and building sectors[23], improving short-term air quality and long-term climate resilience.

Urban green space and compactness are not inherently at odds, but, in practice, one may come at the other's expense at the within-city scale[24,25]. As a recent review states, "while densification policies contribute to the safeguarding of natural spaces at the regional level, they tend to reduce green areas within urban areas"[25]. Nevertheless, strategies to promote both urban green and compactness have been proposed[26,27], highlighting that the two principles can co-occur if planned deliberately[28]. In one proposed framework, ideal levels of greenness vary with density[26].

As evidence accumulates suggesting green-space exposure benefits health[6–9,13], several health-impact-assessment (HIA) studies have sought to quantify premature mortality that could be averted by adding green space in urban environments[29–32]. These HIAs have not considered what level of greenness is attainable for a given level of population density, however. Urban greening may not have a net benefit for public health, for example, if a city block becomes greener at the expense of residential density[33], potentially harming housing affordability and encouraging more motor-vehicle trips. To inform global sustainability targets, such as United Nations Sustainable Development Goal 11 to make cities and human settlements inclusive, safe, resilient and sustainable[34], there is a need for HIA studies estimating health

[1]Scripps Institution of Oceanography, University of California San Diego, San Diego, CA, USA. [2]Department of Environmental and Radiological Health Sciences, Colorado State University, Fort Collins, CO, USA. [3]Irset Institut de Recherche en Santé, Environnement et Travail, UMR-S 1085, Inserm, University of Rennes, EHESP, Rennes, France. [4]State Key Laboratory of Urban and Regional Ecology, Research Center for Eco-Environmental Sciences, Chinese Academy of Sciences, 100085 Beijing, China. [5]Beijing Urban Ecosystem Research Station, Research Center for Eco-Environmental Sciences, Chinese Academy of Sciences, 100085 Beijing, China. [6]University of Chinese Academy of Sciences, 100049 Beijing, China. [7]European Centre for Environment and Health, Regional Office for Europe, World Health Organization, Platz der Vereinten Nationen 1, 53113 Bonn, Germany. [8]World Health Organization (WHO), 20 Avenue Appia, Geneva, Switzerland. [9]Colorado School of Public Health, Colorado State University, Fort Collins, CO, USA. ✉e-mail: mdgarber@ucsd.edu

benefits of urban greening while considering what is achievable for a given population density within the urban area.

Our goal is thus to estimate the number of premature deaths that could be averted annually by greening 15,917 global urban areas to empirically derived levels assumed to be attainable for within-urban-area population density and biome. We stratify analyses by biome because target levels of greenness may vary by biome within urban area.

Methods

Using the square-kilometer gridded-cell pixel as the unit of analysis, we conducted a quantitative HIA to estimate the potential reduction in all-cause premature mortality among adults aged 30 years and older living in 15,917 urban areas worldwide. Specifically, within each urban area's category of population density and biome, we estimated the mortality impact of raising greenness of pixels in the bottom two greenness tertiles to that of the 83rd percentile.

Data sources

Data sources used for this analysis and corresponding web links, as applicable, are described in Table 1.

Urban boundaries. To define distinct urban areas, we used the 2018 dataset of global urban boundaries (GUBs) prepared by Li et al.[35]. This vector-format dataset uses a globally consistent method of defining urban boundaries. The method builds upon the 30-m global artificial impervious area data[35]. The data include 65,462 urban boundaries, each with an area greater than 1 km^2. We call the areas contained within these boundaries urban areas, as the boundaries may not necessarily correspond to the administrative boundaries of cities.

Countries. To define country boundaries, we downloaded the Natural Earth vector dataset at the most detailed scale (1:10 m) using the rnaturalearth R package[36]. We classified countries by income and region using the 2022 World Bank classification[37].

Population and population density. Population density, a measure of population per unit of land area, is among the defining measures of the compactness of an area[38]. To measure population density, we used the LandScan Global dataset of estimated population counts from 2019. This raster-format dataset classifies each gridded cell of the globe with 1 of 9 categories of estimated population counts: 0; 1–5; 6–25; 26–50; 51–100; 101–500; 501–2500; 2501–5000; 5001–185,000[39]. These gridded cells are about 1 square kilometer and are slightly smaller towards the poles[40]. As described further below, our analysis is stratified by urban area. Within an urban area, we assume that grid cells have the same size and thus that each LandScan population category is a category of population density.

To calculate the total population affected by the proposed green-space scenarios, we made two adjustments to these LandScan bounds. First, our preliminary analyses suggested that a simple mean of the two LandScan bounds would yield implausibly high population estimates when summed to the country level. To avoid over-estimating population, we divided each country's United Nations 2019 population estimate (downloaded from the United Nations Data Portal: https://population.un.org/dataportal/; accessed January 18th, 2024) by the sum of its constituent pixels' LandScan upper population bounds. The median value of this quotient, which we call the upper-bound population-correction factor, was 0.32 over all countries. We multiplied each pixel's upper LandScan population bound by its country's correction factor and used the resulting value as the operational upper bound for that pixel's population. We did not correct the lower population bounds.

Second, we restricted the population at risk to adults 30 years old and older (henceforth, adults 30+), as the average minimum age of the cohorts included in the meta-analysis, weighting by cohort population, from which the exposure-response function was estimated (described further below) is 29 years[13]. To do so, we first divided the country's total population by its population of adults 30+ using United Nations population estimates by 5-year age group in 2019. We then multiplied this proportion by the adjusted LandScan category bounds described above. Throughout analyses, we use the mean of these adjusted bounds (i.e., [lower value + upper value]/2) for point estimates and the values of the adjusted bounds themselves for uncertainty intervals.

Mortality. The outcome of interest is non-accidental mortality, which we define as mortality due to all causes except for injury, guided by cohort studies on the topic[41–43]. We gathered the proportions of total deaths due to injury (both unintentional and intentional) by 5-year age group (30–34, 35–39,…, 85+) and country in 2019 along with the all-cause mortality rates in the same strata from the World Health Organization's data portal. Of the 183 countries with age-group-specific all-cause 2019 mortality data, the age-group-specific proportion due to injury in 2019 was missing in 105 (57% of) countries. In countries missing this proportion, we used data from the latest available year before 2019 and after 2009. If no data was available during this period (n, countries = 67; 37% of total), we imputed the country's values using linear regression. In each 5-year age group among the 116 countries with available data, we modeled the proportion of deaths due to injury as a function of World Bank income group and World Bank region (additional detail in Supplementary Notes 1). Using these age-group-stratified models, we imputed the proportion of deaths due to injury among the 67 countries where these data were missing. To consider modeling uncertainty, we re-sampled the imputed proportion for each age-group and country from a normal distribution (mean = predicted value, standard deviation = standard error of predicted value) and calculated the 95% confidence interval as the 2.5th and 97.5th percentiles over 1000 bootstrap replications.

We then calculated non-accidental mortality rates by 5-year age group and country by multiplying the complement of the proportion of deaths due to injury and its corresponding lower and upper confidence limits by the corresponding all-cause mortality rate. We calculated age-standardized non-accidental mortality rates and corresponding confidence intervals by country among adults 30+ as the weighted average of the age-group-specific mortality rates in 5-year age groups, where the weights are the proportions of the global population in the corresponding age groups[44].

Green space and greenness. We define green space as any vegetated land within an urban area, which could be publicly or privately owned and may include but is not limited to parks, landscaped streets, or residential gardens. Green space types will vary widely from place to place in this global analysis, the implications of which we consider further in the discussion section. We define greenness, our primary exposure of interest, as a continuous measure of the level of vegetation of green spaces[45]. We measured greenness using the Normalized Difference Vegetation Index (NDVI), as it is globally available and the evidence linking greenness and mortality from cohort studies is largely expressed in terms of NDVI[13]. We gathered NDVI data from the MODIS NDVI 16-day composite product at a 1 km resolution (MOD13A2 Version 6) in 2019. We used the 1-km spatial resolution to match that of the LandScan global population data. We then calculated the maximum value of NDVI for each pixel in 2019 on the Google Earth Engine platform, following the rationale of Bille et al.[46].

Global biomes. A biome, the largest geographic biotic unit[47], "is an area classified according to the species that live in that location"[48]. "Temperature range, soil type, and the amount of light and water" are some defining characteristics[48]. Examples of biomes include various types of forests, deserts, grasslands, mangroves, rock and ice, and tundra. We used the Ecoregions2017© dataset to classify biomes (Table 1). The vector data classify the world into 846 ecoregions and 14 biomes[49]. A map of biomes appears in Supplementary Fig. 1.

Names of urban areas. The urban-boundary dataset[35] described above does not name the vector features, as the boundaries do not necessarily correspond to municipality boundaries. To facilitate the interpretation of some results, we named these urban areas using two sources: the Pro

Table 1 | Data sources

Data source	Measured construct	Geographic unit	Method of obtaining data (link in table footnote if applicable)	Monetary cost at the time
Global urban boundaries prepared by Li et al.[35]	Boundaries of urban areas	Global urban boundary	Direct download[a]	Free
Natural Earth vector dataset	Boundaries of countries	Country	Using rnaturalearth package[b]	Free
World Bank income and region	Country income level and region	Country	Direct download[c]	Free
LandScan	Gridded population and population density	~1 square-kilometer pixel	Direct download[d]	Free
WHO Data Portal (Mortality)	Age-stratified cause-specific mortality rates	Country	Direct download[e]	Free
MODIS NDVI 16-day composite (MOD13A2 Version 6)	Greenness	~1 square-kilometer pixel	Google Earth Engine (GEE)[f]. The data are also available for download on other data portals[g]	Free
Ecoregions2017©	Biomes	Biome	Direct download[h]	Free
"Pro" version of the World Cities Database created by SimpleMaps.com	Names of cities	Point coordinates of cities	Download after payment[i]	$200 USD
GeoNames dataset of global cities with a population above 1000	Names of cities	Point coordinates of cities	Direct download[j]	Free

[a]http://data.ess.tsinghua.edu.cn/gub.html; accessed March 8th, 2023.
[b]https://www.naturalearthdata.com/downloads/, accessed March 9th, 2023.
[c]https://datahelpdesk.worldbank.org/knowledgebase/articles/906519-world-bank-country-and-lending-groups; accessed June 27, 2024.
[d]https://landscan.ornl.gov; accessed March 8th, 2023.
[e]https://platform.who.int/mortality/themes/theme-details/MDB/all-causes; accessed January 19.
[f] https://developers.google.com/earth-engine/datasets/catalog/MODIS_061_MOD13A2; accessed June 27, 2024.
[g]https://lpdaac.usgs.gov/products/mod13a2v006/; accessed June 27, 2024.
[h]https://ecoregions.appspot.com; accessed March 9th, 2023.
[i]https://simplemaps.com/data/world-cities; Accessed October 9, 2023.
[j]https://public.opendatasoft.com/explore/dataset/geonames-all-cities-with-a-population-1000/; Accessed October 9, 2023.

version of the World Cities Database created by SimpleMaps.com (*N*, cities and towns = 1.95 million when downloaded on October 6th, 2023)[50], and the GeoNames dataset of global cities with a population above 1000 (*N*, cities = 141,121 when downloaded on October 9th, 2023)[51]. Each dataset contains point coordinates (a latitude and longitude value), the city's name, the city's population, and other administrative information. We named GUBs first according to the most populous named city contained within the boundary using city population values from the SimpleMaps.com dataset. If no name was found therein (*N*, missing name = 24,382), we named the city according to the most populous city in the Geonames dataset contained within the GUB. Of the 65,606 GUBs, 46,470 were named with either data source.

We also used the Geonames dataset of cities with a population above 1000 to assess the completeness of the GUB data. Of the 230 countries and territories represented in the GeoNames dataset, 170 had a GUB (Supplementary Notes 2). Of the 141,121 cities in the GeoNames dataset, 52,347 (37%) were contained within a GUB (Supplementary Table 2). Most (83%) of the total population of these cities (using that dataset's city-population figures) was within a GUB (Supplementary Table 2), and this population share was highest in high-income OECD countries (87%) and lowest in low-income countries (53%; Supplementary Table 3). Consistent with this result, the median population of cities missing in the GUB data was higher in low-income (11,466) compared with high-income OECD countries (1504; Supplementary Table 3). The share of Geonames cities contained within a GUB stratified by country appears in Supplementary Table 4.

Combining data sources

We characterized each grid cell at the global scale with values of GUB, population (density), country, non-accidental mortality rate, greenness, and biome. Some datasets were available in raster format (population, NDVI) and some in vector format (urban boundaries, country boundaries, biomes). We re-sampled the NDVI raster dataset to match the resolution of the Landscan raster. We then converted the vector datasets to raster format to populate each LandScan cell with values of global urban boundary, country (and thus corresponding estimated country-level mortality rate, described above), and biome.

We restricted pixels to those in countries with available mortality data and in urban areas with an area greater than 5 km^2 (~5 pixels) and a total population (sum of lower bounds of constituent LandScan pixels) above 1000 to allow for adequate variability in NDVI within population-density categories and to exclude urban areas with very low population, resulting in a final dataset of 1,015,551 pixels located in 15,917 distinct urban areas, 157 countries, and 14 biomes.

Quantitative health-impact assessment

We began the HIA by stratifying pixels by country, biome, urban area, and population-density category such that all calculations are relative to their stratum. That is, for a given pixel, calculations consider only pixels in that pixel's corresponding stratum. Most urban areas (91.3%) were completely contained within one biome. We stratified by biome to ensure results are relative to biome for those urban areas (8.7%) whose boundaries include two or more biomes. We defined the 83rd NDVI percentile within stratum as the target NDVI value. The 83rd percentile is the median of the top greenness tertile (i.e., half-way between the 67th and 100th percentiles) within stratum, and we assume this level of greenness is attainable for that population density in that biome in that urban area. Adding notation for clarity, let $NDVI_{1,j}$ denote this target NDVI value for stratum *j*. Then, for all pixels in the bottom two NDVI tertiles (i.e., below the 67th percentile) of stratum *j*, we calculated the difference, NDVI $difference_{i,j}$, between their actual NDVI value, $NDVI_{0,i,j}$, for pixel *i* in stratum *j*, and their target value using Eq. (1):

$$NDVI\ difference_{i,j} = NDVI_{1,j} - NDVI_{0,i,j} \quad (1)$$

This hypothetical change in greenness—from the pixel's actual NDVI to its target value within stratum of biome, urban area, and population density—is the proposed greening scenario.

To translate this NDVI difference to an estimated number of annual non-accidental deaths prevented, we summarized risk ratios (RRs) from 3 cohort studies relating greenness exposure with non-accidental mortality[41,43,52] that were deemed to have a low risk of bias in a meta-analysis on the topic[13]. We did not use the meta-analyzed risk ratio from that meta-analysis because its endpoint was all-cause mortality[13], and our outcome of interest is non-accidental mortality. Two of the three cohort studies were set in Canadian cities[41,52], while the other was set in Rome, Italy[40]. Their follow-up time ranged from 4 to 22 years. Each adjusted for several potential confounders including age and measures of socioeconomic status. We calculated the weighted mean RR over the 3 studies, $k = 1,2,3$, using Eq. (2):

$$weighted\ mean\ RR = \exp\left(\frac{\sum_{k=1}^{3}\log(RR_k) * w_k}{\sum_{k=1}^{3} w_k}\right) \quad (2)$$

where RR_k is study *k*'s RR, and w_k is proportional to the size of its study population.

The weighted mean RR was 0.954 (95% confidence interval [CI] = 0.944, 0.961).

The unit of change in NDVI exposure within a residential buffer between 250 and 500 meters corresponding to this RR was 0.146, which we calculated using Eq. (3):

$$\text{weighted mean exposure unit of NDVI} = \frac{\sum_{k=1}^{3} exposure\ unit_k * w_k}{\sum_{k=1}^{3} w_k} \quad (3)$$

where $exposure\ unit_k$ is cohort study *k*'s unit of change in NDVI corresponding to its RR, and w_k is again proportional to study *k*'s population size.

In summary, pooling results from these cohort studies[41,43,52], for every 0.146 unit increase in residential exposure to NDVI within a buffer of 250–500 meters, the relative risk of non-accidental mortality decreased about 4.5% (pooled RR = 0.954; 95% CI: 0.944, 0.961). We assume that the area covered by each pixel (about 1 square kilometer) can reasonably approximate the exposure area used by these cohort studies (250–500 m buffer). We then calculated the population attributable fraction (PAF) for pixel *i* in stratum *j*, $PAF_{i,j}$, using Eq. (4)[53]:

$$PAF_{i,j} = 1 - \frac{1}{RR^{\frac{NDVI\ difference_{i,j}}{0.146}}} \quad (4)$$

where the RR is raised to the quantity, $\frac{NDVI\ difference_{i,j}}{0.146}$, to allow it to change multiplicatively per 0.146 of NDVI $difference_{i,j}$.

We estimated both the age-standardized number of non-accidental deaths prevented and the crude (i.e., not adjusted for age) number of non-accidental deaths prevented in each pixel. Each measure provides useful and distinct information. The age-standardized prevented number of non-accidental deaths is useful for comparing prevented mortality between locations holding population age structure constant, and the crude number provides the magnitude of prevented mortality in that location considering its actual age distribution. In pixel *i*, to calculate the age-standardized number prevented, we multiplied the pixel's population (mean of adjusted category bounds, described above), $population_i$, by the pixel's corresponding country's age-standardized non-accidental mortality rate in adults 30+, age − standardized $rate_i$, and multiplied that product by the pixel's PAF, flipping the sign because the risk

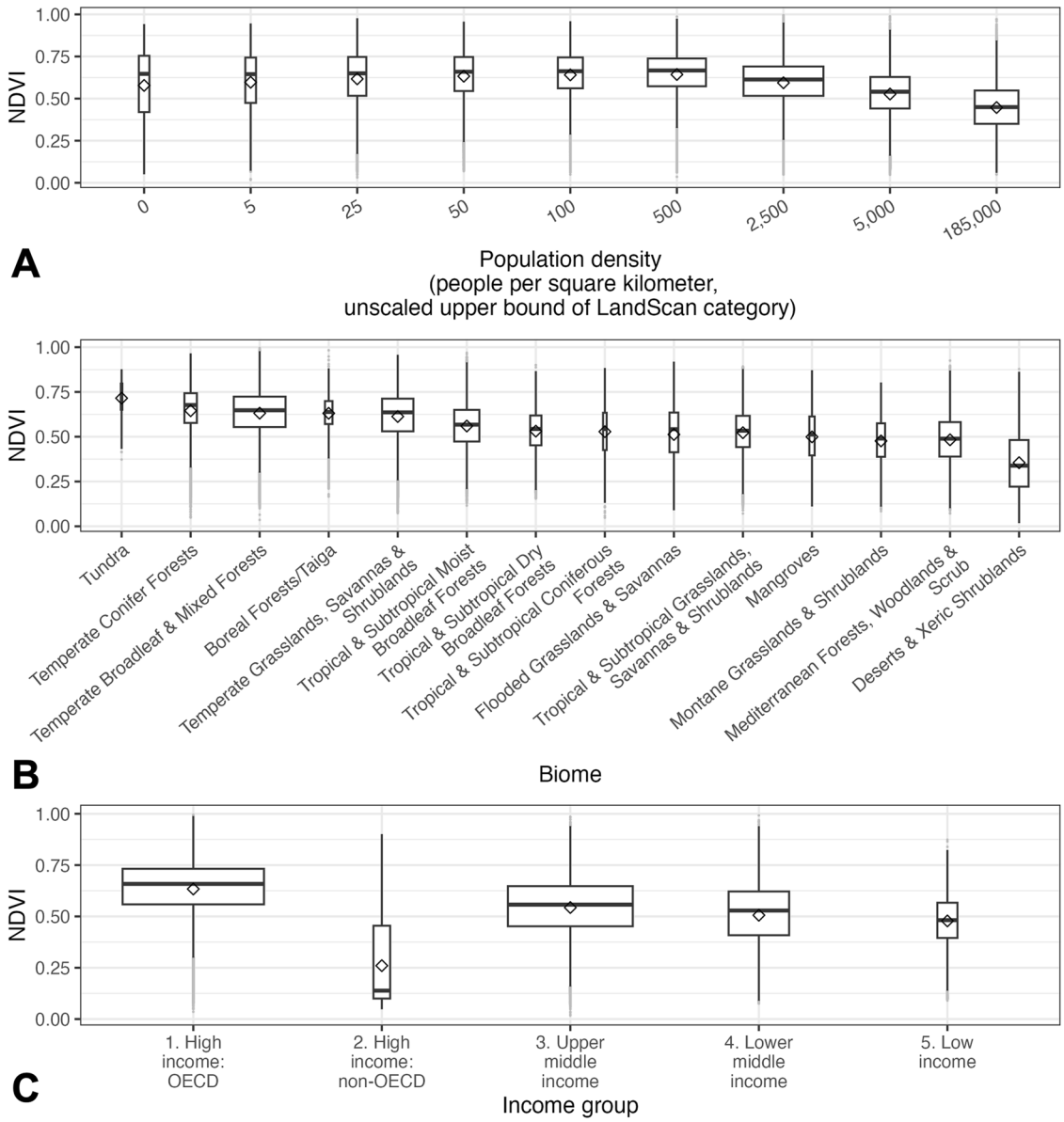

Fig. 1 | Distribution of NDVI by population density, biome, and World Bank income classification. Box-and-whisker plots depicting the distribution of NDVI of pixels plotted by categories of (**A**) density (upper bound of category) per square kilometer, (**B**) biome, and (**C**) World Bank Income category of country. The presented population-density category upper bound is the unadjusted original LandScan value, not the value adjusted for the upper-bound population-correction factor or the proportion of the population 30+. The median in each boxplot is denoted by the horizontal line between the upper and lower sides of the box. The upper side of the box denotes the 75th percentile pixel, and the lower side denotes the 25th percentile pixel. The mean is represented by the diamond shape. The width of each box is proportional to the square root of the number of observations in that category. Whiskers include observed values within 1.5 times the interquartile range (75th percentile–25th percentile) from the lower or upper quartile. Outliers are shaded in gray.

ratio is preventive, as shown by Eq. (5):

$$age-standardized\ number\ of\ non-accidental\ deaths\ prevented_i = population_i * age-standardized\ rate_i * PAF_{i,j} * -1 \quad (5)$$

We calculated the unadjusted number of prevented non-accidental deaths analogously using Eq. (6):

$$crude\ number\ of\ deaths\ prevented_i = population_i * crude\ rate_i * PAF_{i,j} * -1 \quad (6)$$

Uncertainty

We quantified three sources of uncertainty: the population ranges estimated by LandScan (e.g., 5001–185,000 people in a pixel), the pooled RR relating a change in NDVI with non-accidental mortality (95% CI: 0.944, 0.961), and the imputed proportion of mortality due to non-accidental causes in some countries. To consider these sources of uncertainty in our estimates of mortality prevented, we repeated the analysis twice more, once using the pixel's lower adjusted LandScan bound, the weaker RR limit (0.961), and the lower confidence limit of non-accidental mortality and again using the pixel's upper adjusted LandScan bound, the stronger RR limit (0.944), and the upper limit of non-accidental mortality. The resulting lower and upper bounds are our reported 95% uncertainty intervals.

https://doi.org/10.1038/s43247-024-01803-y

Table 2 | Results summarized by population density of pixel, biome, and World Bank income classification of country over the 15,917 urban areas among pixels in the bottom two thirds of the NDVI distribution within stratum (*N*, pixels = 666,095)[a]

Attribute	Affected population[b], millions (lower bound, upper bound)	Crude number of non-accidental deaths[b], estimate (lower bound, upper bound)	NDVI difference: target − actual[a], median (25th, 75th percentiles)	Age-standardized non-accidental death rate prevented per 100,000 population[b], estimate (95% UI)	Crude non-accidental death rate prevented per 100,000 population[b], estimate (95% UI)	Crude number of non-accidental deaths prevented[b], estimate (95% UI)
Total	1423.69 (381.37; 2466.01)	16,383,972 (4,436,450; 28,131,181)	0.09 (0.06, 0.15)	51 (37, 66)	49 (40, 60)	702,956 (151,976; 1,488,762)
Population density (residents per km^2) of pixel, upper bound of LandScan range[c]						
185,000	1223.78 (234.32; 2213.24)	13,883,044 (2,612,736; 25,012,296)	0.12 (0.08, 0.18)	54 (42, 68)	50 (41, 61)	611,050 (96,938; 1,347,925)
5000	77.45 (50.85; 104.06)	949,360 (625,243; 1,252,723)	0.10 (0.06, 0.16)	39 (32, 48)	47 (39, 58)	36,754 (19,581; 60,060)
2500	109.78 (86.24; 133.33)	1,389,945 (1,073,460; 1,671,758)	0.10 (0.06, 0.15)	35 (30, 43)	46 (37, 55)	50,062 (32,177; 73,327)
500	11.73 (9.29; 14.16)	149,904 (116,727; 179,561)	0.08 (0.05, 0.13)	32 (27, 38)	40 (33, 49)	4748 (3084; 6913)
100	0.69 (0.48; 0.89)	8510 (5963; 10,831)	0.07 (0.03, 0.13)	30 (24, 38)	36 (29, 44)	249 (141; 392)
50	0.19 (0.13; 0.25)	2416 (1668; 3099)	0.07 (0.03, 0.12)	29 (23, 37)	36 (29, 43)	69 (39; 110)
25	0.06 (0.05; 0.07)	744 (615; 855)	0.07 (0.03, 0.14)	31 (26, 38)	39 (32, 47)	23 (16; 33)
5	0.00 (0.00; 0.00)	49 (39; 59)	0.07 (0.02, 0.13)	30 (26, 37)	38 (32, 46)	1 (1; 2)
Biome of pixel						
Temperate Broadleaf & Mixed Forests	491.69 (163.21; 820.18)	5,941,283 (1,955,228; 9,699,220)	0.10 (0.06, 0.15)	43 (33, 54)	53 (42, 64)	261,421 (67,916; 529,002)
Tropical & Subtropical Moist Broadleaf Forests	367.42 (72.47; 662.37)	3,925,285 (763,586; 7,084,682)	0.12 (0.08, 0.19)	65 (50, 82)	52 (42, 63)	189,634 (30,736; 419,306)
Deserts & Xeric Shrublands	146.26 (32.00; 260.51)	1,528,438 (325,477; 2,763,527)	0.09 (0.05, 0.13)	47 (35, 59)	36 (29, 45)	52,692 (9336; 117,163)
Tropical & Subtropical Dry Broadleaf Forests	105.73 (17.10; 194.37)	1,198,015 (192,582; 2,224,362)	0.10 (0.06, 0.15)	58 (44, 74)	47 (38, 58)	49,678 (6458; 113,425)
Mediterranean Forests, Woodlands & Scrub	81.92 (28.74; 135.11)	973,283 (335,562; 1,557,535)	0.10 (0.06, 0.15)	38 (30, 48)	49 (39, 60)	40,548 (11,093; 80,422)
Temperate Grasslands, Savannas & Shrublands	75.22 (32.37; 118.07)	999,523 (433,347; 1,546,074)	0.08 (0.05, 0.13)	41 (31, 51)	48 (39, 58)	36,051 (12,508; 68,858)
Tropical & Subtropical Grasslands, Savannas & Shrublands	67.08 (12.80; 121.36)	760,886 (149,905; 1,411,501)	0.09 (0.06, 0.14)	60 (42, 78)	41 (35, 52)	27,794 (4520; 63,277)
Mangroves	23.54 (4.18; 42.90)	262,260 (46,745; 490,220)	0.10 (0.06, 0.15)	56 (43, 70)	45 (38, 57)	10,564 (1588; 24,242)
Montane Grasslands & Shrublands	20.65 (3.75; 37.54)	240,703 (47,065; 441,254)	0.09 (0.05, 0.13)	58 (43, 74)	43 (36, 54)	8965 (1348; 20,342)
Flooded Grasslands & Savannas	16.93 (5.02; 28.84)	199,916 (58,465; 332,069)	0.11 (0.06, 0.17)	85 (63, 108)	68 (51, 82)	11,432 (2568; 23,532)
Temperate Conifer Forests	13.42 (5.37; 21.48)	167,020 (67,430; 264,100)	0.08 (0.05, 0.13)	42 (28, 55)	44 (35, 54)	5938 (1900; 11,703)
Boreal Forests/Taiga	7.25 (2.63; 11.87)	114,069 (41,834; 186,168)	0.09 (0.05, 0.14)	47 (37, 58)	65 (49, 81)	4693 (1293; 9594)
Tropical & Subtropical Coniferous Forests	5.55 (1.45; 9.66)	57,807 (15,223; 103,650)	0.11 (0.07, 0.18)	61 (45, 77)	55 (42, 70)	3037 (613; 6800)
Tundra	0.12 (0.06; 0.19)	1860 (824; 2892)	0.05 (0.03, 0.10)	30 (27, 36)	40 (36, 47)	49 (20; 91)

Table 2 (continued) | Results summarized by population density of pixel, biome, and World Bank income classification of country over the 15,917 urban areas among pixels in the bottom two thirds of the NDVI distribution within stratum (*N*, pixels = 666,095)[a]

Attribute	Affected population[b], millions (lower bound, upper bound)	Crude number of non-accidental deaths[b], estimate (lower bound, upper bound)	NDVI difference: target − actual[a], median (25th, 75th percentiles)	Age-standardized non-accidental death rate prevented per 100,000 population[b], estimate (95% UI)	Crude non-accidental death rate prevented per 100,000 population[b], estimate (95% UI)	Crude number of non-accidental deaths prevented[b], estimate (95% UI)
World Bank income classification of country						
High income: OECD	297.00 (124.67; 469.33)	3,892,340 (1,602,444; 6,047,194)	0.09 (0.05, 0.13)	33 (25, 41)	58 (43, 71)	171,058 (53,244; 333,918)
High income: non-OECD	16.10 (4.65; 27.54)	103,440 (30,690; 180,847)	0.05 (0.03, 0.08)	23 (20, 28)	15 (14, 19)	2463 (664; 5128)
Upper middle-income	595.72 (177.94; 1013.51)	6,420,613 (1,923,077; 10,784,912)	0.11 (0.07, 0.17)	49 (40, 60)	47 (38, 57)	277,934 (68,072; 574,162)
Lower middle-income	407.06 (66.98; 747.14)	4,756,041 (795,453; 8,747,781)	0.10 (0.06, 0.15)	67 (53, 85)	51 (41, 62)	206,116 (27,422; 466,411)
Low income	107.80 (7.12; 208.47)	1,211,538 (84,786; 2,370,448)	0.09 (0.06, 0.14)	62 (51, 80)	42 (36, 52)	45,385 (2575; 109,144)

[a]As described in the text, pixels are stratified by country, biome, urban area, and population-density category. Each pixel's target NDVI value is the 83rd percentile NDVI value within stratum. The NDVI difference (target-actual) and corresponding mortality impact is only assessed among those pixels in the bottom two NDVI tertiles within stratum.
[b]Affected population is restricted to adults 30 years old and older and pixels in the bottom two NDVI tertiles, as described in the text.
[c]We emphasize that this measure of population density describes the pixel (about 1 square kilometer), not the urban area. An urban area may contribute to more than one population-density category.

Reporting summary

Further information on research design is available in the Nature Portfolio Reporting Summary linked to this article.

Results

Distribution of NDVI and population density over urban areas

The distribution of NDVI among the 1,015,551 pixels by category of population density, biome and World Bank income group is presented in Fig. 1. The number of distinct population-density categories within a given urban area ranged from 1 to 9 with a median of 3 (Supplementary Fig. 2). Including within-urban-area variation, median NDVI was roughly the same throughout the lower six population density categories until the 100–500 residents-per-km^2 category, after which average NDVI fell with increasing population density (Fig. 1). This trend was broadly consistent when stratified by biome (Supplementary Fig. 3) with some exceptions such as Deserts & Xeric Schrublands, where the median NDVI was lowest where population density was lowest.

Although median NDVI was lowest in the most population-dense pixels (Panel A, Fig. 1), these pixels also presented the largest opportunity to raise NDVI. The median NDVI difference (the difference between the target and actual NDVI values within stratum of country, global urban boundary, biome, and population-density category among pixels in the lower two NDVI tertiles) was highest in the most population-dense pixels (median NDVI difference: 0.12; 25th–75th percentile: 0.08, 0.18; Table 2).

Non-accidental deaths prevented

Overall, we estimated that 702,956 (95% uncertainty interval (UI): 151,976; 1,488,762) non-accidental premature deaths would be prevented annually by the greening scenario (Table 2), corresponding to an estimated 49 (95% UI: 40, 60) deaths per 100,000 adults 30+. This estimated prevented mortality corresponds to about 4% (UI: 3%, 5%) of the estimated 16,383,972 (UI: 4,436,450; 28,131,181) deaths that occurred in the adult 30+ population living in the bottom two NDVI tertiles of the 15,917 included urban areas. The estimated prevented mortality was highest in the most population-dense pixels (5001–185,000 residents per km^2), whether measured by the age-standardized annual premature death rate prevented per 100,000 adults 30+ (54 [95 % UI: 42, 68)] or by the corresponding crude measure without adjusting for age structure (50 [95% UI: 41, 61]). Variation in the prevented rate between population-density categories was starker in the age-standardized measure.

Summarizing results by biome, the age-standardized prevented premature death rate ranged from 30 (95% UI: 28, 36) in the sparsely populated Tundra to 65 (95% UI: 49, 82) per 100,000 adults 30+ in the more populous Tropical & Subtropical Moist Broadleaf Forests (Table 2). When age structure is not considered, the prevented death rate was lowest in Deserts & Xeric Shrublands (36 [29,45]) and highest in Flooded Grasslands & Savannas (68 [50,82]) per 100,000 adults 30+. Low and lower-middle-income countries had higher age-adjusted prevented death rates (62 [95% UI: 51, 80] and 67 [95% UI: 52, 85], respectively) than higher-income countries (e.g., (33 [25,41] in high-income OECD countries; Table 2). This trend did not generally hold when population age structure was not considered, presumably because crude mortality rates are higher in higher-income countries because of their older populations on average.

Figures 2–4 rank GUBs (top 50) by their age-standardized premature mortality rate prevented grouped by GUB population, where population bounds in the figure correspond to the summed mean adjusted values of constituent LandScan pixels. Figures 5–7 rank included countries by their estimated age-standardized premature mortality rate prevented, grouped by the country's World Bank income classification. We have posted results for all urban areas and countries on a public website: https://michaeldgarber.github.io/global-ndvi-pop/results-by-city-country.html.

Discussion

At the nexus of public health and urban planning, there is increasing agreement that both compactness and green space are beneficial for public

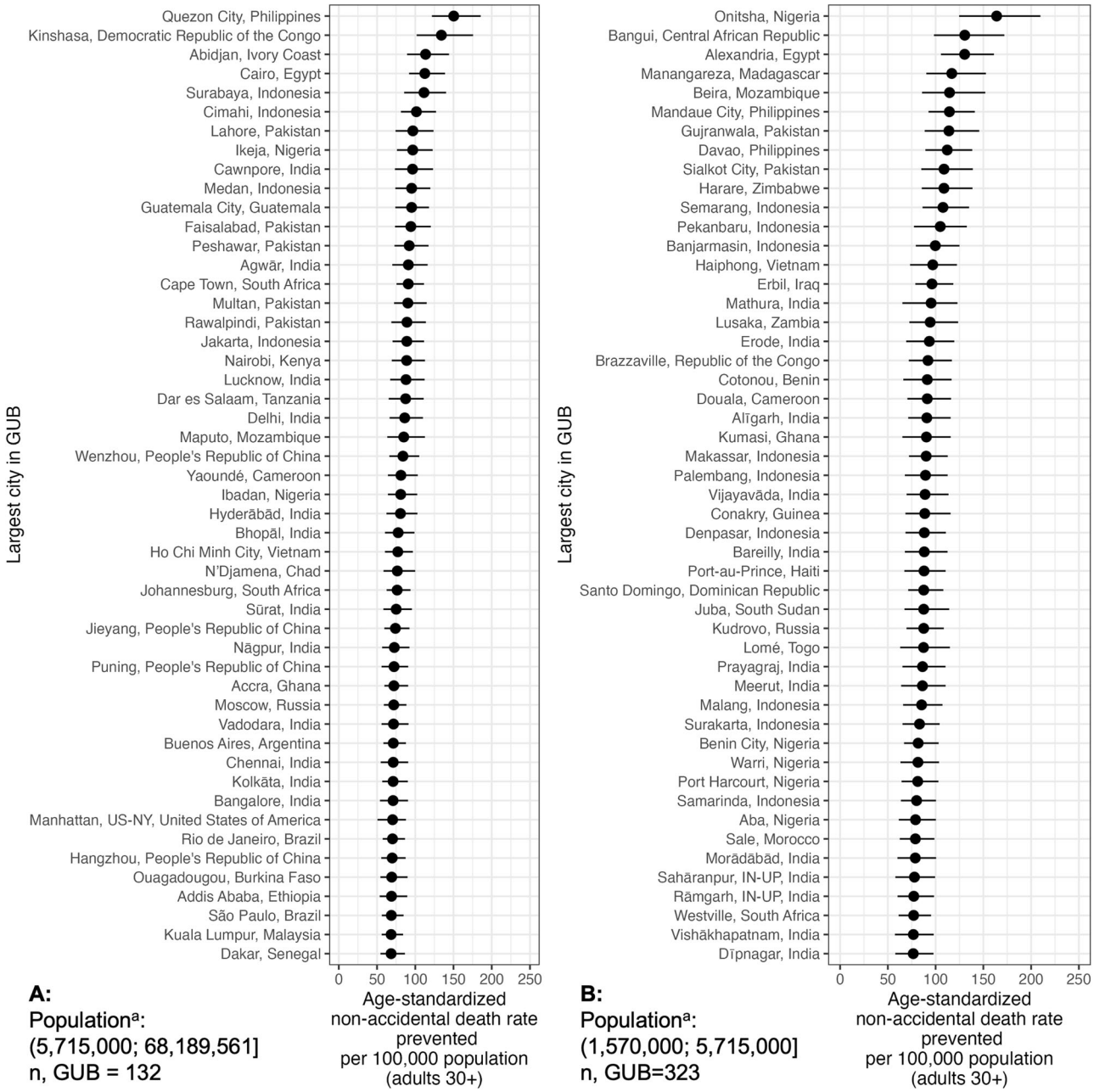

Fig. 2 | Top 50 global urban areas (GUBs) ranked in descending order by the estimated age-standardized non-accidental death rate prevented per 100,000 population (adults 30+) by the greening scenario among the most populous urban areas. The areas are grouped by population (**A**: 5,715,001; 68,189,561; **B**: 1,570,000; 5,715,000). [a]The bounds of the population ranges correspond to the summed adjusted mean values of constituent LandScan pixels. Population groups are adapted from the Atlas of Urban Expansion Volume 1[72]. The horizontal lines denote the 95% uncertainty interval. GUBs are named according to the largest-population city contained therein. As described in the text, not all GUBs were named by the city-name data sources. Unnamed GUBs are named in the figure using their ID in the GUB dataset (e.g., 16266) prepared by Li et al.[35].

health with co-benefits for climate change mitigation and adaptation[13,16,54]. We have conducted a global health impact assessment estimating mortality prevented by greening 15,917 urban areas according to achievable levels of greenness for within-area population density and biome. Compared with other large-scale studies estimating health impacts of greening cities using similar methods[29,30], a unique aspect of our approach is that we empirically consider what level of greenness is achievable given constraints of the local context. By targeting empirically derived greenness levels within category of population density within the urban area, our analysis acknowledges that certain levels of greenness (those of a forest, for example) may not be feasible in locations with high population densities[24,25]. Nevertheless, an important result of our analysis is that even in areas of high population density, there is considerable potential for additional greenness and thus for preventing premature mortality. In fact, on a per-population basis, we estimated that preventable mortality was highest in the most population-dense areas.

Assumptions and limitations

This study makes several assumptions and carries limitations that should be considered when interpreting the results. The most important assumption is that the meta-analyzed risk ratio from these three cohort studies, which were set in Canada and Italy, is a valid measure of the effect of green space on non-accidental mortality in the 15,917 urban areas around the world. The effect of green-space exposure on mortality could depend, for example, on population density, biome, climate, development status of the country[55], or

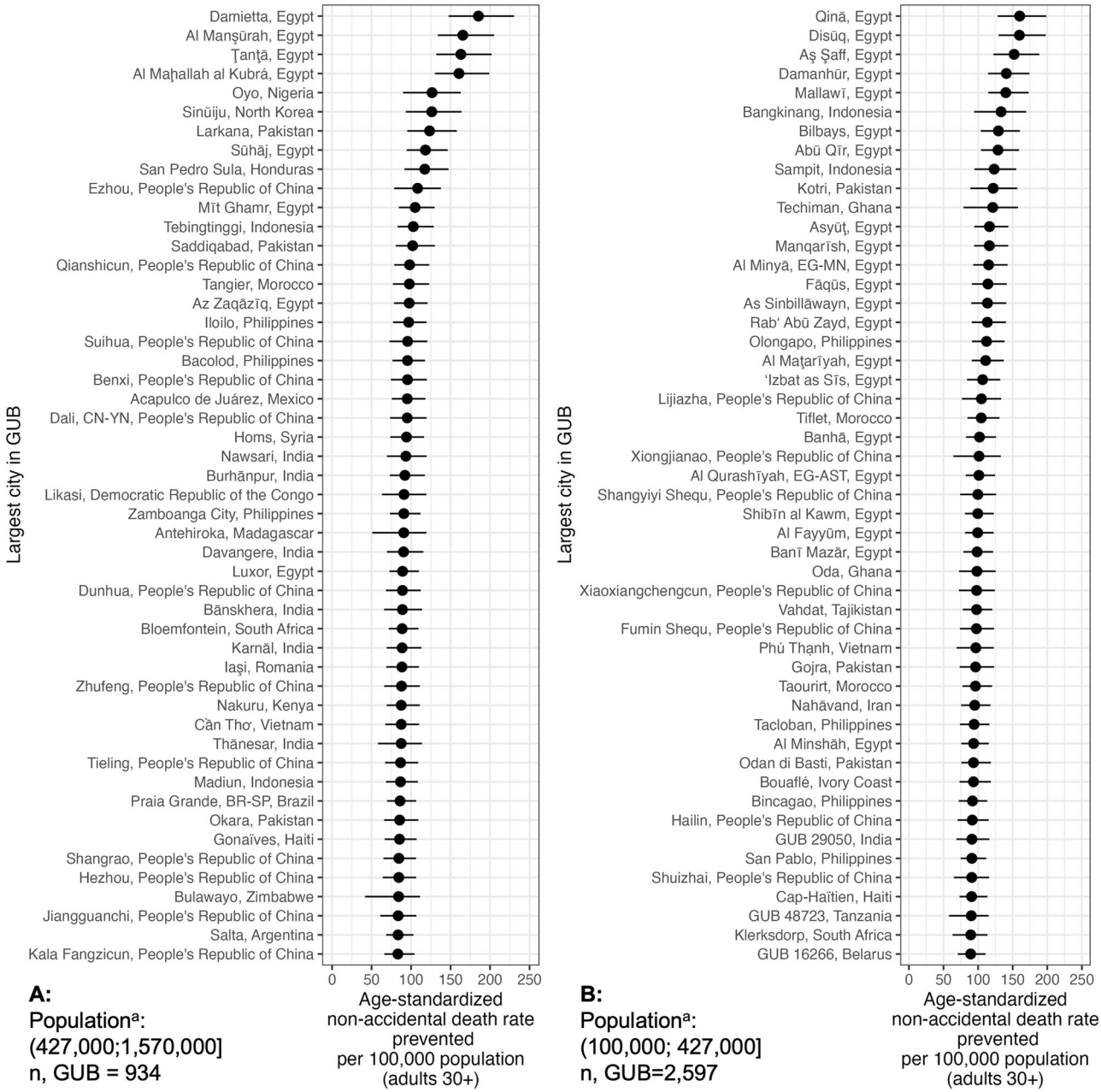

Fig. 3 | Top 50 global urban areas (GUBs) ranked in descending order by the estimated age-standardized non-accidental death rate prevented per 100,000 population (adults 30+) by the greening scenario among moderately populated urban areas. The areas are grouped by population (**A**: 427,001; 1,570,000; **B**: 100,000; 427,000). [a]The bounds of the population ranges correspond to the summed adjusted mean values of constituent LandScan pixel. Population groups are adapted from the Atlas of Urban Expansion Volume 1[72]. The horizontal lines denote the 95% uncertainty interval. GUBs are named according to the largest-population city contained therein. As described in the text, not all GUBs were named by the city-name data sources. Unnamed GUBs are named in the figure using their ID in the GUB dataset (e.g., 16266) prepared by Li et al.[35].

any of a range of other potential effect modifiers[9]. While this assumption of transportability is strong, evidence supports a fairly consistent effect of green space on mortality. In the meta-analysis by Rojas et al. on the effect of green space exposure on all-cause mortality, the 9 risk ratios of the included studies—which are set in North America (4), Europe (3), Australia (1), and Asia [China] (1)—range from 0.88 to 0.99, and the most common value is 0.92. More research is needed to represent Africa, Latin America, and other regions of Asia, but the evidence to date supports the notion that green space can prevent premature mortality in various settings.

Related to the potential variability of the effect of green space on health is the variability of the costs of adding green space across the world. In desert settings where water is scarce and drought is persistent such as the Middle East or the Southwestern United States, urban greening efforts should be weighed against their environmental consequences such as water consumption. The desert city of Las Vegas, Nevada, United States (population: 650,000), for example, receives 90 percent of its water from the Colorado River[56], and that river basin has been in an extended drought over the last two decades[57]. In response, local authorities have instituted seasonal water restrictions, golf-course water budgets, a grass-replacement program, and water waste penalties[56]. In such a water-constrained setting, urban greening may be tailored to the natural landscape by using native or drought-resistant plants[32] and may be informed by guidance on techniques for greening settlements in arid lands in a sustainable manner[58,59]. It is also worth noting that natural landscapes without abundant vegetation may confer health

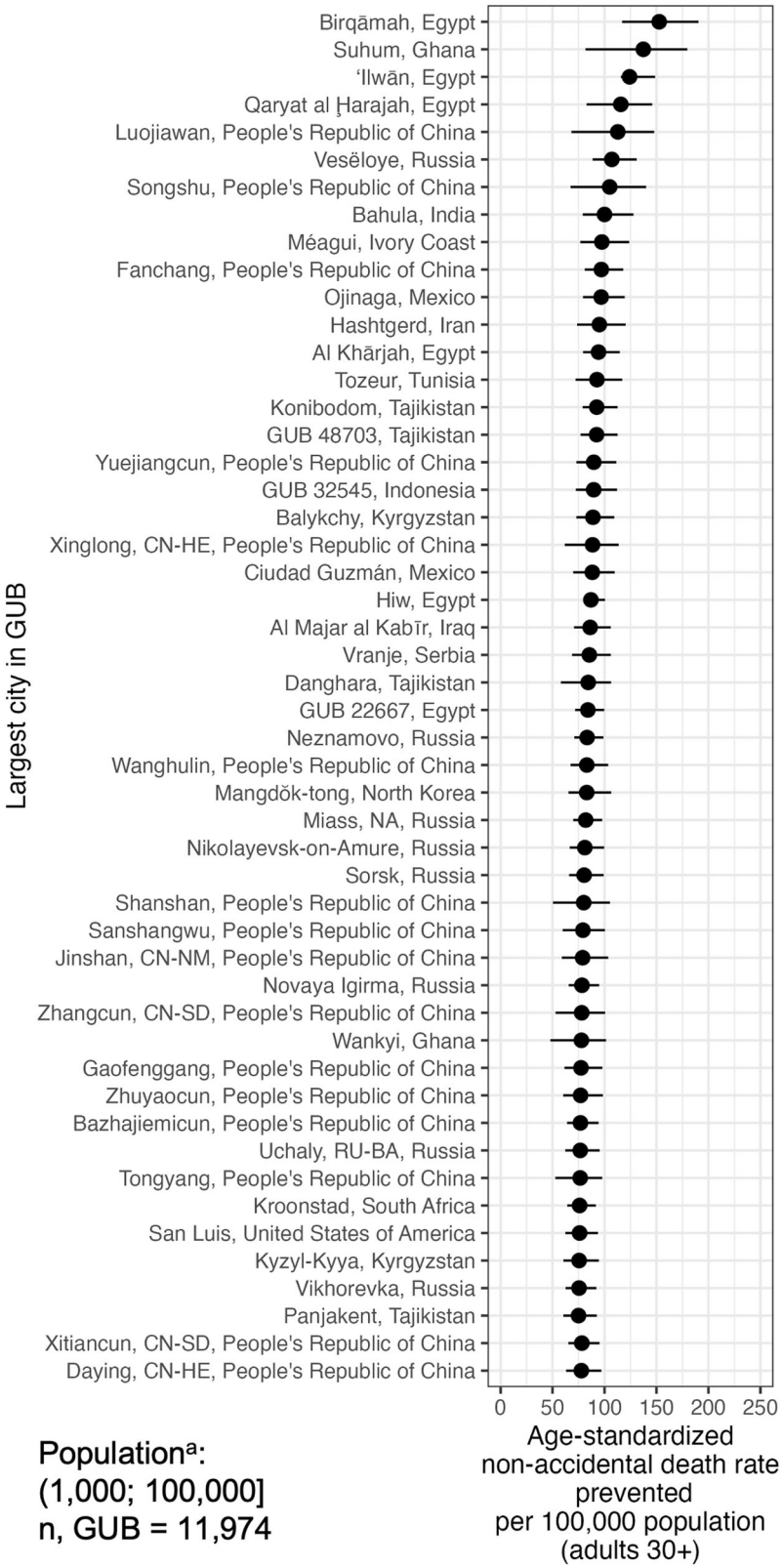

Fig. 4 | Top 50 global urban areas (GUBs) ranked in descending order by the estimated age-standardized non-accidental death rate prevented per 100,000 population (adults 30+) by the greening scenario among the least populous urban areas (population: 1000; 100,000). [a]The bounds of the population ranges correspond to the summed adjusted mean values of constituent LandScan pixels. Population groups are adapted from the Atlas of Urban Expansion Volume 1[72]. The horizontal lines denote the 95% uncertainty interval. GUBs are named according to the largest-population city contained therein. As described in the text, not all GUBs were named by the city-name data sources. Unnamed GUBs are named in the figure using their ID in the GUB dataset (e.g., 16266) prepared by Li et al.[35].

benefits[60]. Exposure to desert landscapes dominated by rock and minerals, for example, may improve mental health (e.g., by relieving stress, promoting feelings of well-being, or focusing attention) in such a way similar to that of a verdant forest[60], but epidemiologic research on this topic is limited. If we exclude from the global total Desert & Xeric Shrublands and Tundra, two biomes in particular for which greenness may be an incomplete measure of the salubrity of the natural landscape[60], the total number of estimated premature deaths prevented decreases by about 8% to 649,805 (calculated using values in Table 2).

To a degree, our analysis considers the possibility that the meaning of a greening intervention will vary from one urban area to another[61], as the proposed scenario's target level of greenness is always relative to that urban

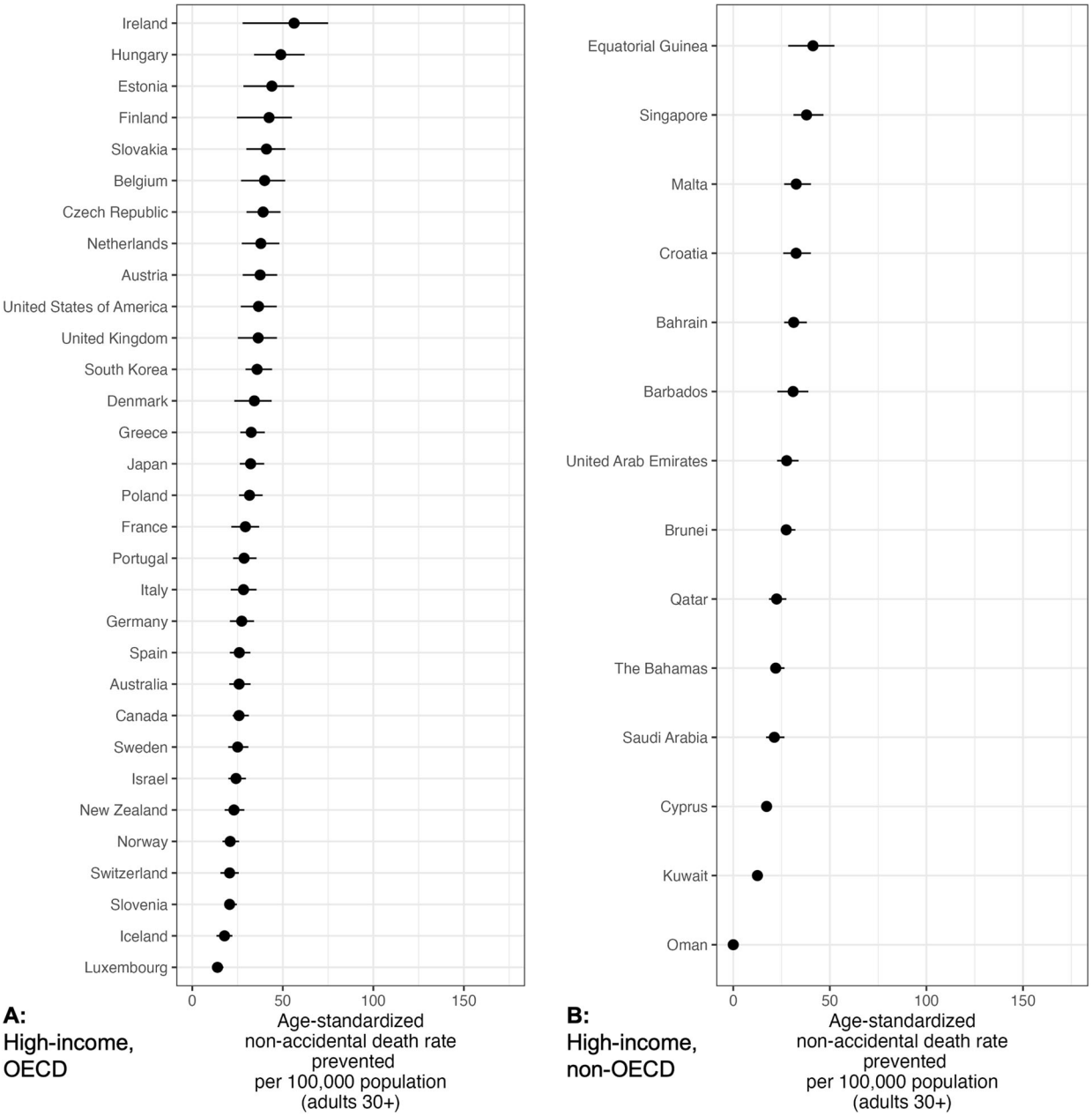

Fig. 5 | High-income countries ranked in descending order by their estimated age-standardized non-accidental death rate prevented per 100,000 population (adults 30+) by the greening scenario. Panel **A** displays high-income OECD countries, and panel **B** displays high-income non-OECD countries. The horizontal lines denote the 95% uncertainty interval. OECD, Organization for Economic Cooperation and Development.

location. At the same time, our methods cannot discern the type of greenness, only its NDVI value[45]. The target greenness in the area may reflect the greenness of a highly irrigated private golf course, for example, the environmental costs of which may outweigh its public-health benefit, or that of a public park landscaped with native drought-resistant plants, which may have a greater and more sustainable return on public health. To increase the chance that the target level of greenness is attainable for that area and does not represent an unrealistic exception, we used the 83rd percentile of NDVI within stratum of urban area and population density as the target value rather than, say, the 95th percentile.

Another important consideration, as has been articulated previously[32], is the time scale for these health benefits to manifest. Depending on the greenness-health pathway[6], mortality benefits may appear relatively quickly (e.g., if greenness prevents acute heat-related mortality) or may take decades to bear fruit (e.g., if greenness exposure encourages habitual physical activity, preventing cardiovascular disease). The risk ratios in the cohort studies represent an average over the life course comparing the risk of death from non-accidental causes in those with more versus less residential greenness exposure. Our aim is to quantify the potential health benefits under this imaginary counterfactual scenario if the populations under consideration had been exposed to this level of greenness over their life course. The last limitation pertaining to the validity of the effect measure is the potential for confounding. The cohort studies from which the risk ratios were obtained controlled for many possible confounders[41,43,52], including the possibility that higher-income individuals may live near greener areas, but residual or unmeasured confounding remains possible. If such a confounding bias resulted in an overestimate of the strength of the effect, the results from this HIA would also be over-estimated.

Other limitations pertain to the data sources for population, mortality, and GUBs. We used a gridded population model (LandScan) because of its

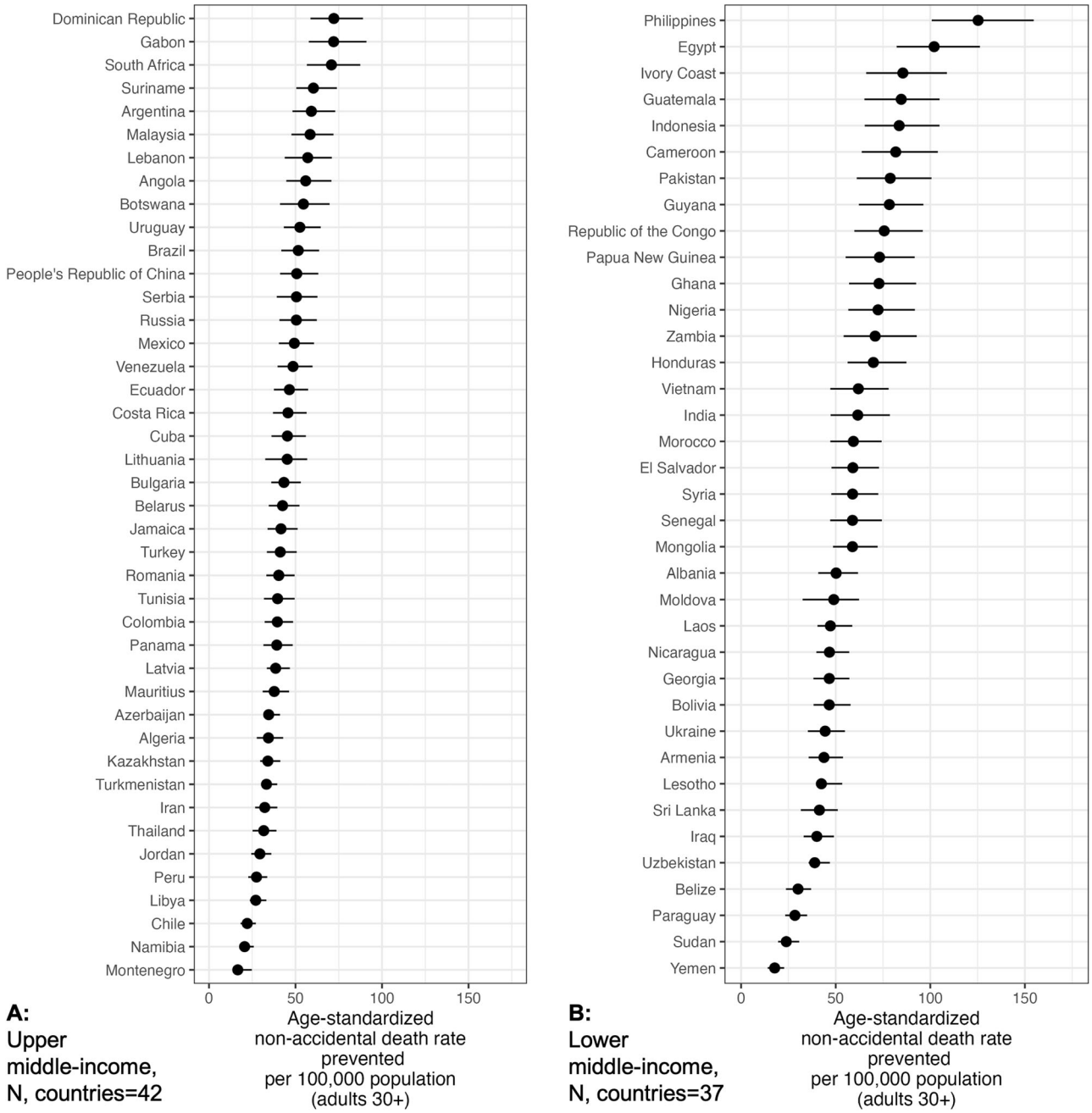

Fig. 6 | Middle-income countries ranked in descending order by their estimated age-standardized non-accidental death rate prevented per 100,000 population (adults 30+) by the greening scenario. Panel **A** displays upper middle-income countries, and panel **B** displays lower middle-income countries. The horizontal lines denote the 95% uncertainty interval.

high spatial resolution and globally consistent coverage. Its limitation here was the wide range between bounds, particularly at the highest population-density range, leading to concern that populations would be over-estimated., We adjusted each pixel's LandScan value considering country-level population data to ensure that the population values were within a plausible range, but the resulting estimates remain imprecise.

The mortality data sources also have limitations. First, as described, age-stratified injury mortality data are not available from WHO for all countries; we have integrated the uncertainty from the imputation model into confidence intervals of the results. Second is our inherent assumption of no within-country variation in the mortality rates, as only country-level mortality data were available. Estimates of mortality rates at a within-country scale are not available in a harmonized fashion globally[62], so this assumption is difficult to overcome. Violations of this assumption may not consequentially affect summary estimates (such as those presented in Table 2), where the country-level average mortality rates may suffice. The validity of estimates at the level of the urban area, however, is more susceptible to violations of this assumption, considering well-documented within-country variability in mortality in many countries[63–65]. This analysis could be replicated as data on non-accidental mortality become more complete for all countries and for urban areas within countries.

Finally, the dataset of GUBs spans 65,462 urban areas but is not globally comprehensive (Supplementary Notes 2). As the GUB data are less complete in low- and low-middle-income countries, absolute estimates of prevented mortality may be relatively under-estimated in those countries. Without knowledge of the distribution of NDVI within strata of population density in the cities excluded from the GUB data, it is difficult to speculate as

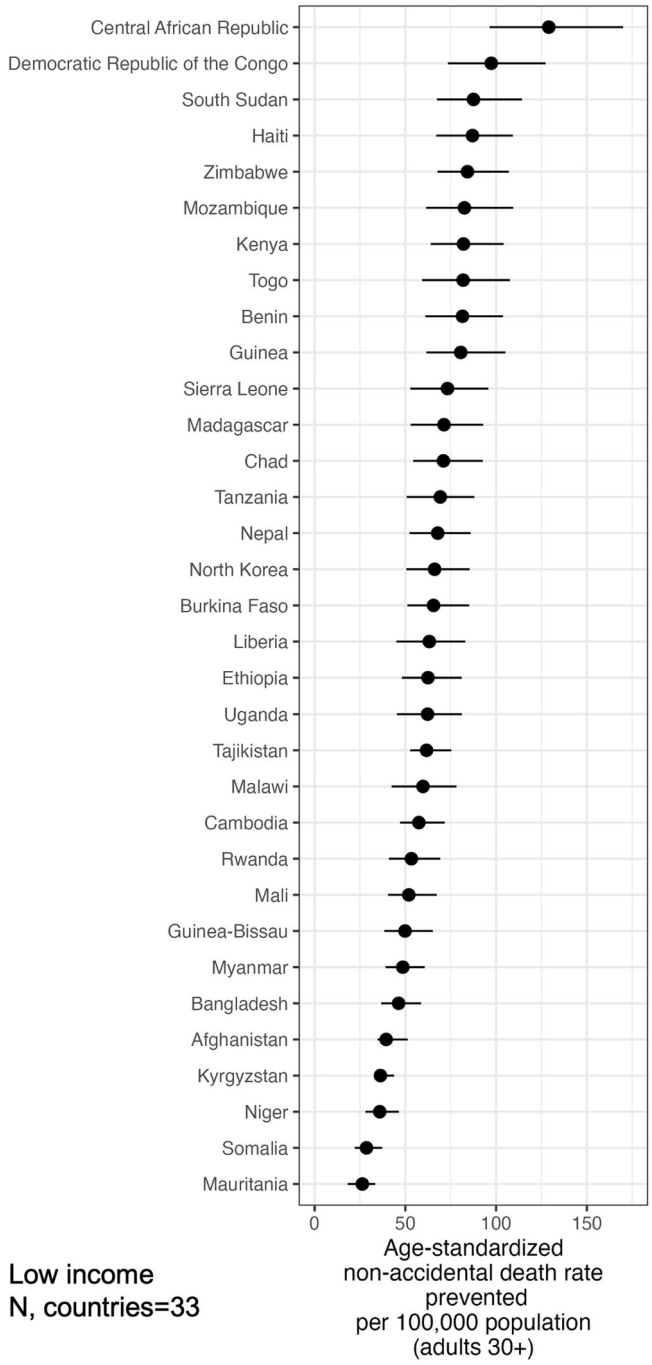

Fig. 7 | Low-income countries ranked in descending order by their estimated age-standardized non-accidental death rate prevented per 100,000 population (adults 30+) by the greening scenario. The horizontal lines denote the 95% uncertainty interval.

to the potential direction of any selection bias in the per-population estimates of prevented mortality.

Implications for public health

With these limitations and assumptions in mind, the findings from this health impact assessment have important implications for urban planning and public health. The analysis suggests that there is a large potential to add greenness to urban areas even within the most population-dense areas, and that this added greenness could have a considerable preventive impact on premature mortality (about 700,000 annual prevented deaths estimated here among an estimated 1.4 billion adults affected by the proposed scenario). For comparison, the global burden attributable to unsafe drinking-water, sanitation and hygiene was estimated to be 1.4 million deaths in 2019[66]. The analysis highlights that compactness and greenness need not be mutually exclusive[27,28]. The results also have important implications for global health equity, as the estimated prevented mortality was highest on an age-standardized, per-population basis in lower middle-income and low-income countries. This result is a function of both the relatively high NDVI difference in these countries between the actual and target greenness scenarios and their relatively higher baseline age-standardized mortality rates.

Urban planners and policymakers may consider strategies to promote both green space and density at the neighborhood scale while mitigating potential adverse environmental consequences of adding green space such as water consumption. For example, cities could aim to add green infrastructure like street trees, green roofs, and parks even in the densest areas. Building codes could incentivize green roofs and walls. In water-constrained settings, drought-resistant plants could be used for this green infrastructure. Zoning policies could allow mixed-use development that integrates housing with greenspace. Transportation planning could promote development of protected pedestrian and cycling networks and replace on- and off-street parking with green space[32,54]. To monitor progress, cities could track indicators of greenness such as type and characteristics of green spaces, tree canopy cover and NDVI by neighborhood[67]. Policies should prioritize equitable distribution of urban green space to ensure benefits across socioeconomic gradients. In closing, results suggest that green-space interventions can improve public health even in dense urban areas. The health impact modeling approach used here can help inform context-specific urban greening strategies and quantify their potential health benefits.

Data availability

All data gathered for this analysis were publicly available at no monetary cost at the time we downloaded them except for one dataset of city names, as described in Table 1. Output data[68] to replicate all results except for Figs. 2–4 can be found here: https://figshare.com/projects/Potential_of_greenness_to_prevent_premature_mortality_in_15_917_urban_areas_considering_within-area_population_density_and_ecological_zone/221455. We do not provide data to re-produce Figs. 2–4 because their requisite data rely in part on the purchased dataset of city names, which we do not have license to publicly share.

Code availability

We used Google Earth Engine to retrieve NDVI data and used R for all other data management and analysis. In R, we used terra[69], sf[70], and the tidyverse[71] for most tasks. Our R code is publicly available on GitHub (https://github.com/michaeldgarber/global-ndvi-pop). Specifically, code to create Table 2 is here (https://github.com/michaeldgarber/global-ndvi-pop/blob/main/scripts/tables-main-text.R), and code to produce figures is here (https://github.com/michaeldgarber/global-ndvi-pop/blob/main/scripts/figures-main-text.R).

Received: 12 April 2024; Accepted: 17 October 2024;
Published online: 02 November 2024

References

1. World Bank Group. Urban development—overview. World Bank. https://www.worldbank.org/en/topic/urbandevelopment/overview (2023).
2. de Sa, T. H. et al. Urban design is key to healthy environments for all. *Lancet Glob. Health* **10**, e786–e787 (2022).
3. Nieuwenhuijsen, M. J. Urban and transport planning pathways to carbon neutral, liveable and healthy cities; a review of the current evidence. *Environ. Int.* **140**, 105661 (2020).
4. Lowe, M. et al. City planning policies to support health and sustainability: an international comparison of policy indicators for 25 cities. *Lancet Glob. Health* **10**, e882–e894 (2022).

5. Giles-Corti, B. et al. City planning and population health: a global challenge. *Lancet* **388**, 2912–2924 (2016).
6. Jimenez, M. P. et al. Associations between nature exposure and health: a review of the evidence. *Int. J. Environ. Res. Public Health* **18**, 1–19 (2021).
7. Nieuwenhuijsen, M. J., Khreis, H., Triguero-Mas, M., Gascon, M. & Dadvand, P. Fifty shades of green: pathway to healthy urban living. *Epidemiology* **28**, 63–71 (2017).
8. WHO. *Urban Green Spaces and Health: A Review of Evidence* (World Health Organization Regional Office for Europe, 2016).
9. Besser, L. M. & Lovasi, G. S. Human physical health outcomes influenced by contact with nature. In *Nature-Based Solutions for Cities* (eds McPhearson, T., Kabisch, N. & Frantzeskaki, N.) 167–191 (Edward Elgar Publishing, 2023).
10. Diener, A. & Mudu, P. How can vegetation protect us from air pollution? A critical review on green spaces' mitigation abilities for air-borne particles from a public health perspective—with implications for urban planning. *Sci. Total Environ.* **796**, 148605 (2021).
11. Sha, Z. et al. The global carbon sink potential of terrestrial vegetation can be increased substantially by optimal land management. *Commun. Earth Environ.* **3**, 8 (2022).
12. Braubach, M., Kendrovski, V., Jarosinska D. & Mudu P. *Green and Blue Spaces and Mental Health: New Evidence and Perspectives for Action* (World Health Organization Regional Office for Europe, 2021).
13. Rojas-Rueda, D., Nieuwenhuijsen, M. J., Gascon, M., Perez-Leon, D. & Mudu, P. Green spaces and mortality: a systematic review and meta-analysis of cohort studies. *Lancet Planet. Health* **3**, e469–e477 (2019).
14. Wang, H. C. Prioritizing compactness for a better quality of life: the case of U.S. cities. *Cities* **123**, 103566 (2022).
15. Stevenson, M. et al. Land use, transport, and population health: estimating the health benefits of compact cities. *Lancet* **388**, 2925–2935 (2016).
16. Moreno, C., Allam, Z., Chabaud, D., Gall, C. & Pratlong, F. Introducing the "15-Minute City": sustainability, resilience and place identity in future post-pandemic cities. *Smart Cities* **4**, 93–111 (2021).
17. Logan, T. M. et al. The x-minute city: measuring the 10, 15, 20-minute city and an evaluation of its use for sustainable urban design. *Cities* **131**, 103924 (2022).
18. Sallis, J. F. et al. Physical activity in relation to urban environments in 14 cities worldwide: a cross-sectional study. *Lancet* **387**, 2207–2217 (2016).
19. Brand, C. et al. The climate change mitigation impacts of active travel: evidence from a longitudinal panel study in seven European cities. *Glob. Environ. Change* **67**, https://doi.org/10.1016/j.gloenvcha.2021.102224 (2021).
20. Schuetz, J. *To Improve Housing Affordability, We Need Better Alignment of Zoning, Taxes, and Subsidies* (Brookings, 2023).
21. Jenks, M. & Burgess, R., eds. *Compact Cities: Sustainable Urban Forms for Developing Countries* (Spon Press, 2000).
22. Brownstone, D. & Golob, T. F. The impact of residential density on vehicle usage and energy consumption. *J. Urban Econ.* **65**, 91–98 (2009).
23. Mostafavi, N., Heris, M., Gándara, F. & Hoque, S. The relationship between urban density and building energy consumption. *Buildings* **11**, 455 (2021).
24. Haaland, C. & van den Bosch, C. K. Challenges and strategies for urban green-space planning in cities undergoing densification: a review. *Urban For. Urban Green.* **14**, 760–771 (2015).
25. Madureira, H. & Monteiro, A. Going green and going dense: a systematic review of compatibilities and conflicts in urban research. *Sustainability* **20**, https://doi.org/10.3390/su131910643 (2021).
26. Sanches, P., Lemes de Oliveira, F. & Celani, G. Green and compact: a spatial planning model for knowledge-based urban development in peri-urban areas. *Sustainability* **13**, 13365 (2021).
27. Artmann, M., Inostroza, L. & Fan, P. Urban sprawl, compact urban development and green cities. How much do we know, how much do we agree? *Ecol. Indic.* **96**, 3–9 (2019).
28. McDonald, R. I. et al. Denser and greener cities: green interventions to achieve both urban density and nature. *People Nat.* **5**, 84–102 (2023).
29. Brochu, P., Jimenez, M. P., James, P., Kinney, P. L. & Lane, K. Benefits of increasing greenness on all-cause mortality in the largest metropolitan areas of the United States within the past two decades. *Front. Public Health* **10**, 841936 (2022).
30. Barboza, E. P. et al. Green space and mortality in European cities: a health impact assessment study. *Lancet Planet. Health* **5**, e718–e730 (2021).
31. Kondo, M. C. et al. Health impact assessment of Philadelphia's 2025 tree canopy cover goals. *Lancet Planet. Health* **4**, e149–e157 (2020).
32. Garber, M. D. et al. Impact of native-plants policy scenarios on premature mortality in Denver: a quantitative health impact assessment. *Environ. Int*. 108050 https://doi.org/10.1016/j.envint.2023.108050 (2023).
33. Richardson, E. A. et al. Green cities and health: a question of scale? *J. Epidemiol. Community Health* **66**, 160–165 (2012).
34. Sustainable Development Goals. *Goal 11: Make Cities Inclusive, Safe, Resilient and Sustainable* (United Nations Sustainable Development, 2023).
35. Li, X. et al. Mapping global urban boundaries from the global artificial impervious area (GAIA) data. *Environ. Res Lett.* **15**, 094044 (2020).
36. Massicotte, P., South, A. & Hufkens, K. rnaturalearth: World Map Data from Natural Earth. https://CRAN.R-project.org/package=rnaturalearth (2023).
37. World Bank Country and Lending Groups. World Bank Data Help Desk. https://datahelpdesk.worldbank.org/knowledgebase/articles/906519-world-bank-country-and-lending-groups (2023).
38. Diez-Roux, A. V. What is urban health? Defining the geographic and substantive scope. In *Urban Public Health: A Research Toolkit for Practice and Impact* (eds Lovasi, G. S., Diez Roux, A. V. & Kolker, J.) 3–26 (Oxford University Press, 2020).
39. Oak Ridge National Laboratory (ORNL). LandScan Viewer—Oak Ridge National Laboratory. https://landscan.ornl.gov/ (2022).
40. Oak Ridge National Laboratory (ORNL). About LandScan. https://landscan.ornl.gov/about (2023).
41. Crouse, D. L. et al. Urban greenness and mortality in Canada's largest cities: a national cohort study. *Lancet Planet. Health* **1**, e289–e297 (2017).
42. James, P., Hart, J. E., Banay, R. F. & Laden, F. Exposure to greenness and mortality in a nationwide prospective cohort study of women. *Environ. Health Perspect.* **124**, 1344–1352 (2016).
43. Orioli, R. et al. Exposure to residential greenness as a predictor of cause-specific mortality and stroke incidence in the Rome longitudinal study. *Environ. Health Perspect.* **127**, 027002 (2019).
44. The Global Health Observatory. *Age-standardized Mortality Rate (Per 100 000 Population)* (World Health Organization, 2024).
45. de la Martinez, A. I. & Labib, S. M. Demystifying normalized difference vegetation index (NDVI) for greenness exposure assessments and policy interventions in urban greening. *Environ. Res.* **220**, 115155 (2023).
46. Bille, R. A., Jensen, K. E. & Buitenwerf, R. Global patterns in urban green space are strongly linked to human development and population density. *Urban For. Urban Green.* **86**, 127980 (2023).
47. Biome. *Definition, Map, Types, Examples, & Facts* | Britannica https://www.britannica.com/science/biome (2023).
48. National Geographic Education. Encyclopedic Entry: Biomes. https://education.nationalgeographic.org/resource/resource-library-biomes (2023).
49. Dinerstein, E. et al. An ecoregion-based approach to protecting half the terrestrial realm. *BioScience* **67**, 534–545 (2017).
50. World Cities Database. Simplemaps.com. https://simplemaps.com/data/world-cities (2023).

51. Opendatasoft. Geonames—all cities with a population >1000. https://public.opendatasoft.com/explore/dataset/geonames-all-cities-with-a-population-1000/ (2023).
52. Villeneuve, P. J. et al. A cohort study relating urban green space with mortality in Ontario, Canada. *Environ. Res.* **115**, 51–58 (2012).
53. Lash, T. L. & Rothman, K. J. Measures of occurrence. In *Modern Epidemiology* 4th edn (eds Lash, T. L., VanderWeele, T. J. & Haneuse, S. R.) 53–77 (Wolters Kluwer, 2021).
54. Iungman, T. et al. The impact of urban configuration types on urban heat islands, air pollution, CO2 emissions, and mortality in Europe: a data science approach. *Lancet Planet. Health* **8**, e489–e505 (2024).
55. Kusumaning Asri, A. et al. Is green space exposure beneficial in a developing country? *Landsc. Urban Plan.* **215**, 104226 (2021).
56. Las Vegas Valley Water District. Drought and conservation measures. https://www.lvvwd.com/conservation/measures/index.html (2024).
57. The Economist. The American West is drying up. *The Economist*. https://www.economist.com/united-states/the-american-west-is-drying-up/21803608 (2024).
58. Yang, J. & Wang, Z. H. Planning for a sustainable desert city: the potential water buffering capacity of urban green infrastructure. *Landsc. Urban Plan.* **167**, 339–347 (2017).
59. He, B., Wang, S., Guo, L. & Wu, X. Aridity change and its correlation with greening over drylands. *Agric. For. Meteorol.* **278**, 107663 (2019).
60. Li, H. et al. Beyond "bluespace" and "greenspace": a narrative review of possible health benefits from exposure to other natural landscapes. *Sci. Total Environ.* **856**, 159292 (2023).
61. Taylor, L. & Hochuli, D. F. Defining greenspace: multiple uses across multiple disciplines. *Landsc. Urban Plan.* **158**, 25–38 (2017).
62. Garber, M. D., Benmarhnia, T., De Nazelle, A., Nieuwenhuijsen, M. & Rojas-Rueda, D. The epidemiologic case for urban health: conceptualizing and measuring the magnitude of challenges and potential benefits. *F1000Res* **13**, 950 (2024).
63. Bilal, U. et al. Life expectancy and mortality in 363 cities of Latin America. *Nat. Med.* **27**, 463–470 (2021).
64. Schnake-Mahl, A. S. et al. Heterogeneity in disparities in life expectancy across US metropolitan areas. *Epidemiology* **33**, 890–899 (2022).
65. Benjamins, M. R., Silva, A., Saiyed, N. S. & De Maio, F. G. Comparison of all-cause mortality rates and inequities between Black and White populations across the 30 most populous US cities. *JAMA Netw. Open* **4**, e2032086 (2021).
66. World Health Organization. *Burden of Disease Attributable to Unsafe Drinking-Water, Sanitation and Hygiene, 2019 Update* (World Health Organization, 2023).
67. Lobe Ekamby, E. S. H. & Mudu, P. How many trees are planted in African cities? Expectations of and challenges to planning considering current tree planting projects. *Urban Sci.* **6**, 59 (2022).
68. Garber, M. Pixel-level output: health-impact assessment of greening relative to population density and biome. https://doi.org/10.6084/M9.FIGSHARE.27080455.V3 (2024).
69. Hijmans, R. J., Bivand, R., Pebesma, E. & Sumner, M. D. terra: Spatial Data Analysis. https://CRAN.R-project.org/package=terra (2023).
70. Pebesma, E. Simple features for R: standardized support for spatial vector data. *R. J.* **10**, 439 (2018).
71. Wickham, H. et al. Welcome to the Tidyverse. *JOSS* **4**, 1686 (2019).
72. Angel et al. *Atlas of Urban Expansion—2016 Edition.* NYU Urban Expansion Program at New York University, UN-Habitat, and the Lincoln Institute of Land Policy; 2016. https://www.lincolninst.edu/publications/other/atlas-urban-expansion-2016-edition (2023).

Acknowledgements

Where authors are identified as staff of the World Health Organization, the authors alone are responsible for the views expressed in this article, and they do not necessarily represent the decisions, policy, or views of the World Health Organization.

Author contributions

All authors read and approve of the final text. Specific author contributions follow. Michael D. Garber: conceptualization, methodology, software, formal analysis, investigation, data curation, writing—original draft, writing—review & editing, visualization; Tarik Benmarhnia: conceptualization, methodology, writing—review & editing, supervision, project administration; Weiqi Zhou: methodology, data curation, writing—review & editing; Pierpaolo Mudu: conceptualization, methodology, writing—review & editing; David Rojas-Rueda: conceptualization, methodology, writing—review & editing; investigation, data curation, supervision, project administration.

Competing interests

The authors declare no competing interests.

Additional information

Supplementary information The online version contains supplementary material available at https://doi.org/10.1038/s43247-024-01803-y.

Correspondence and requests for materials should be addressed to Michael D. Garber.

Peer review information *Communications Earth and Environment* thanks Mohammad Javad Zare Sakhvidi and the anonymous reviewers for their contribution to the peer review of this work. Primary Handling Editors: Heike Langenberg and Mengjie Wang. A peer review file is available.